Published in final edited form as:
Cell Metab. 2009 February ; 9(2): 165–176. doi:10.1016/j.cmet.2009.01.002.

Molecular Mechanisms of Hepatic Steatosis and Insulin Resistance in the AGPAT2 Deficient Mouse Model of Congenital Generalized Lipodystrophy

Víctor A. Cortés[1], **David E. Curtis**[1,2], **Suja Sukumaran**[3,4], **Xinli Shao**[3,4], **Vinay Parameswara**[4], **Shirya Rashid**[1,7], **Amy R. Smith**[1], **Jimin Ren**[5], **Victoria Esser**[4], **Robert E. Hammer**[6], **Anil K. Agarwal**[3,4], **Jay D. Horton**[1,6], and **Abhimanyu Garg**[3,4]

1 *Department of Molecular Genetics, University of Texas Southwestern Medical Center at Dallas, Dallas, TX*

2 *Department of Surgery, University of Texas Southwestern Medical Center at Dallas, Dallas, TX*

3 *Division of Nutrition and Metabolic Diseases,* [3] *Center for Human Nutrition, University of Texas Southwestern Medical Center at Dallas, Dallas, TX*

4 *Department of Internal Medicine, University of Texas Southwestern Medical Center at Dallas, Dallas, TX*

5 *Department of Advanced Imaging, University of Texas Southwestern Medical Center at Dallas, Dallas, TX*

6 *Department of Biochemistry,* [6] *Division of Gastroenterology, Department of Internal Medicine, University of Texas Southwestern Medical Center at Dallas, Dallas, TX*

SUMMARY

Mutations in 1-acylglycerol-3-phosphate-O-acyltransferase 2 (*AGPAT2*) cause congenital generalized lipodystrophy. To understand the molecular mechanisms underlying the metabolic complications associated with AGPAT2 deficiency, *Agpat2* null mice were generated. *Agpat2*$^{-/-}$ mice develop severe lipodystrophy affecting both white and brown adipose tissue, severe insulin resistance, diabetes, and hepatic steatosis. The expression of lipogenic genes and rates of *de novo* fatty acid biosynthesis were increased ~4-fold in *Agpat2*$^{-/-}$ mouse livers. The mRNA and protein levels of monoacylglycerol acyltransferase isoform 1 were markedly increased in the livers of *Agpat2*$^{-/-}$ mice suggesting that the alternative monoacylglycerol pathway for triglyceride biosynthesis is activated in the absence of AGPAT2. Feeding a fat-free diet reduced liver triglycerides by ~50% in *Agpat2*$^{-/-}$ mice. These observations suggest that both dietary fat and hepatic triglyceride biosynthesis via a novel monoacylglycerol pathway may contribute to hepatic steatosis in *Agpat2*$^{-/-}$ mice.

*Correspondence: Abhimanyu Garg, M.D., Division of Nutrition and Metabolic Diseases, Center for Human Nutrition, Department of Internal Medicine, University of Texas Southwestern Medical Center, 5323 Harry Hines Blvd., Dallas, TX 75390, U.S.A., Ph: 214-648-2895, Fax: 214-648-0553, E-mail: E-mail: Abhimanyu.garg@UTSouthwestern.edu.
[7]Current address: Department of Medicine, McMaster University Hamilton, ON, Canada

Keywords

AGPAT; LPAAT; MGAT; phosphatidic acid phosphatases; acyltransferase; phospholipids; lipodystrophy; hepatic steatosis

INTRODUCTION

The 1-acylglycerol-3-phosphate-O-acyltransferases (AGPATs) are members of the acyltransferase family of enzymes with ten putative isoforms based on amino acid sequence homology (Agarwal et al., 2006; Agarwal et al., 2003; Agarwal et al., 2007; Cao et al., 2006; Leung, 2001; Li et al., 2003; Tang et al., 2006; Ye et al., 2005). AGPATs catalyze the conversion of lysophosphatidic acid (LPA, 1-acylglycerol-3-phosphate) to phosphatidic acid (PA, 1,2 diacylglycerol-3-phosphate) by esterifying a fatty acyl group at the *sn*-2 position of the glycerol backbone and thus play a critical role in the biosynthesis of glycerophospholipids and triacylglycerols (TGs) from glycerol-3-phosphate (Leung, 2001; West et al., 1997). Few of these AGPATs have additional acyltransferase activity (Table S1).

The biological relevance of the different AGPAT isoforms remains largely unknown except for AGPAT2 and AGPAT6/GPAT4 (Agarwal and Garg, 2003; Beigneux et al., 2006; Chen et al., 2008; Vergnes et al., 2006). A role for AGPAT2 in TG synthesis and adipocyte biology has emerged since we discovered mutations in *AGPAT2* that cause an autosomal recessively inherited form of congenital generalized lipodystrophy (CGL) type 1 (Agarwal et al., 2002). Patients with CGL are born with near complete absence of adipose tissue and are prone to develop metabolic complications associated with insulin resistance, such as impaired glucose tolerance, diabetes, hypertriglyceridemia, and hepatic steatosis early in life (Agarwal and Garg, 2006; Garg, 2004). High expression of *AGPAT2* in the adipose tissue may explain the lack of adipose tissue in CGL (Agarwal et al., 2002); however, whether the lack of AGPAT2 activity causes lipodystrophy by impairing TG synthesis in the adipocytes or by affecting adipocyte differentiation (Gale et al., 2006) remains unclear. Furthermore, the underlying molecular mechanisms involved in the development of metabolic complications in these patients have not been elucidated. Therefore, to better understand the molecular basis of the metabolic complications due to AGPAT2 deficiency, we generated *Agpat2* null mice and characterized the biochemical and molecular alterations related to the metabolic complications observed in these mice.

RESULTS

Gene Knockout Strategy and Phenotypic Characterization

The strategy used to disrupt *Agpat2* in mice is shown in Figure 1A. A targeting vector containing the neomycin-resistance gene was used to replace a portion of the proximal promoter and exons 1–4 of *Agpat2*. The mouse genotype was confirmed by PCR using genomic DNA (Figure S1A) and the absence of the AGPAT2 mRNA transcript was confirmed using real-time quantitative PCR (Figure S1B). Furthermore, total AGPAT activity was reduced by ~90% in the liver homogenates as measured by conversion of ^{3}H-LPA to ^{3}H-PA (Figure 1B). Matings between *Agpat2*$^{+/-}$ mice produced offspring born in the expected Mendelian 1:2:1 ratio; however ~80% of the *Agpat2*$^{-/-}$ pups died by 3 wk of age. Equal numbers of male and female *Agpat2*$^{-/-}$ mice survived past weaning and had body weights similar to littermate gender-matched wild-type mice (Table 1). The majority of mice that did not reach weaning died during the first week of life. The exact cause of the increased mortality is not known, but two likely contributors are: 1) hyperglycemia resulting in volume depletion, which we could document as early as day 1 after birth (data not shown); and 2) hypothermia, which could occur as a result of lack of body fat.

Lipodystrophic Features

The characterization of the *Agpat2*$^{-/-}$ mice revealed some interesting features in addition to those previously observed in human CGL. Both male and female *Agpat2*$^{-/-}$ mice had a complete absence of white and brown adipose tissue. Whole body ^{1}H-magnetic resonance spectroscopy showed that *Agpat2*$^{-/-}$ mice had 2% body fat compared to 24–29% in the wild type mice (Figure S2). MR imaging (Figure 1C) revealed subcutaneous and intra-abdominal fat in the wild type mice but total lack of these depots in the *Agpat2*$^{-/-}$ mice.

Compared to the age-matched wild type mice, dissection of 8–10 wk old *Agpat2*$^{-/-}$ male and female mice revealed generalized organomegaly including enlarged kidneys (mean and SD; 0.96 ± 0.1 g vs. 1.3 ± 0.1 g, respectively; $P<0.05$), spleens (0.09 ± 0.02 g vs. 0.17 ± 0.05 g, respectively; $P<0.05$), and elongated small intestines (29.2 ± 4.9 cm vs. 41.2 ± 7.9 cm, respectively; $P<0.05$) (Figure S3). The liver weight was more than two times larger in both genders of *Agpat2*$^{-/-}$ mice (Table 1) and liver histology revealed hepatic steatosis (Figures S4 and S5).

The *Agpat2*$^{-/-}$ mice also had markedly enlarged pancreatic islets as seen with hematoxylin and eosin staining (Figure S6). Immunostaining with anti-insulin and anti-glucagon antibodies showed that the enlarged islets were composed of excess of (cells, without significant changes in (cells (Figure S6).

Metabolic Complications—There were modest gender differences in the severity of the hepatic steatosis and hypertriglyceridemia. Male *Agpat2*$^{-/-}$ mice had 6.4-fold higher liver TG concentrations than wild type males but in female *Agpat2*$^{-/-}$ mice the liver TG content was only increased 2.1-fold (Table 1). Plasma TG concentrations were also significantly elevated in the males but not in female *Agpat2*$^{-/-}$ mice (Table 1).

Severe insulin resistance and diabetes mellitus, additional hallmarks of CGL, were recapitulated in both genders of *Agpat2*$^{-/-}$ mice with markedly elevated plasma glucose and insulin levels (Table 1). Plasma free fatty acid (FFA) concentrations were unchanged in male *Agpat2*$^{-/-}$ mice compared to the wild type mice and were significantly lower in the *Agpat2*$^{-/-}$ female mice (Table 1).

Energy Expenditure and Activity Studies

Energy and water consumption, CO_2 production, O_2 consumption, and respiratory exchange ratios (RER) were determined in the wild type and *Agpat2*$^{-/-}$ mice over 72 h in metabolic cages and were adjusted for the 5.7% increase in lean body mass of the *Agpat2*$^{-/-}$ mice (Figure 1D–G). The *Agpat2*$^{-/-}$ mice consumed 85% more energy and 3.7 times more water than the wild type mice during the light period (Figure 1D and E). These differences were maintained in the dark period although they were less pronounced. The near absence of plasma leptin (Table 1) in *Agpat2*$^{-/-}$ mice was likely responsible for the extreme hyperphagia. The knockout mice also consumed 24% more O_2 and emitted 22% more CO_2 than the wild type mice. (Figure 1F and G). The RER was significantly reduced in the knockout mice; particularly during the dark phase suggesting preferential metabolism of fat or a defect in the metabolism of carbohydrates (Figure 1H). Interestingly, the daily excursions in the RER were blunted in the knockout mice, indicating a failure to utilize the ingested carbohydrate as the predominant energy source in the feeding period (Figure 1I). Compared to the wild type mice, *Agpat2*$^{-/-}$ mice had reduced activity (Figure S7A and B) especially during the dark cycle possibly due to leptin deficiency which is associated with reduced locomotor activity (Mesaros et al., 2008).

Molecular Basis of Hepatic Steatosis and Insulin Resistance

To investigate the molecular basis of the insulin resistance, the mRNA and protein levels of insulin receptor (IR), insulin receptor substrate (IRS)-1 and IRS-2 were measured in livers of *Agpat2*$^{-/-}$ mice. While the mRNA levels of the IR and IRS-1 were essentially unchanged, IRS-2 mRNA levels were significantly reduced (60–70%) in both sexes of *Agpat2*$^{-/-}$ mice (Table 2). However, IR (40%), IRS-1 (30%), and IRS-2 (85%) protein levels were significantly reduced in *Agpat2*$^{-/-}$ mouse livers (Figure 2A and B). These results provide a potential mechanism by which insulin signaling in the livers of AGPAT2 deficient mice is impaired.

To study the molecular basis of hepatic steatosis, we measured the mRNA levels of genes involved in fat and glucose metabolism (Table 2). First, we determined whether there was a compensatory increase in the expression of other confirmed and putative *Agpat* genes in *Agpat2*$^{-/-}$ livers. The mRNA levels of AGPAT1 were modestly increased (1.7-fold) in the *Agpat2*$^{-/-}$ males but not in the females. AGPAT3 was slightly increased in both *Agpat2*$^{-/-}$ sexes, whereas AGPAT4 expression remained undetectable. AGPAT5 was increased (1.6-fold) only in *Agpat2*$^{-/-}$ male mice. AGPAT6/GPAT4 and AGPAT7/LPEAT2 were not significantly changed, but interestingly, AGPAT8/ALCAT1 was increased by 4.6 and 1.6-fold, in *Agpat2*$^{-/-}$ males and females, respectively. However, total AGPAT enzymatic activity as measured by the conversion of ^{3}H-LPA to PA was still reduced by ~90% in the liver homogenates of the *Agpat2*$^{-/-}$ mice compared to wild type mice (Figure 1B), confirming that AGPAT2 is responsible for the majority of this activity in the murine liver.

We next determined whether TG accumulation in the livers of *Agpat2*$^{-/-}$ mice occurred preferentially through the glycerol-3-phosphate pathway, the monoacylglycerol (MAG) pathway, or whether dietary TGs were contributing via chylomicron remnant uptake through receptor mediated endocytosis (Figure 2C). The mRNA level of the enzyme catalyzing the first step in glycerol-3-phosphate pathway, glycerol-3-phosphate acyltransferase 1 (GPAT1), was increased by 4.7-fold; however, the mRNA levels of the enzyme catalyzing the final TG assembly in this pathway, diacylglycerol (DAG) acyltransferase (DGAT)-2 remained unchanged. The mRNA expression of DGAT-1 was undetectable. On the other hand, the mRNA expression of a key enzyme involved in an alternative pathway of TG biosynthesis, MAG acyltransferase (MGAT)-1, was markedly upregulated by 48-fold in males and by 25-fold in the female *Agpat2*$^{-/-}$ mice livers. Similarly, the MGAT1 protein levels were increased by 7.3 and 5.4-fold in the livers of *Agpat2*$^{-/-}$ males and females mice, respectively (Figure 2D). The expression of MGAT2 mRNA was undetectable.

MGATs convert MAGs to DAGs, which can be further acylated by DGATs to form TGs (Figure 2C). However, LPA needs to be dephosphorylated to MAG before it can be used as a substrate. Therefore, we investigated whether various phosphatases potentially capable of dephosphorylating LPA to MAG were also upregulated. These enzymes include two types of phosphatidic acid phosphatases (PAPs): Type 1, which include lipins 1, 2 and 3 and Type 2, which include lipid phosphate phosphatases (LPPs), 1, 2 and 3 (Brindley, 2004; Brindley and Waggoner, 1998; Carman and Han, 2006; Donkor et al., 2007). Recent data suggest that lipins can dephosphorylate PA but have no significant activity for LPA (Donkor et al., 2007). On the other hand, LPPs show less substrate preference and can dephosphorylate both LPA and PA (Brindley and Waggoner, 1998).

Our data revealed that in male and female *Agpat2*$^{-/-}$ mice, hepatic mRNA levels of LPP1, isoform 1, were increased by 2.0 and 1.5-fold; LPP2 by 3.4 and 2.0- fold; and lipin 3 by 2.6- and 2.1-fold, respectively (Table 2). Interestingly, lipins 1 and 2 were increased only in *Agpat2*$^{-/-}$ females.

In the livers of male and female *Agpat2*$^{-/-}$ mice, the mRNA levels of lipogenic genes involved in fatty acid synthesis, ATP citrate lyase (5.1 and 3.1-fold), acetyl-coenzyme A carboxylase (ACC)-1 (5.5 and 3.9-fold), fatty acid synthase (FAS) (9.9 and 4.7-fold), elongation of very long chain fatty acids, family member 6 (ELOVL6) (9.3 and 4.9-fold), and stearoyl-coenzyme A desaturase (SCD)-1 (5.7 and 4.2-fold), were increased. There was also a robust, ~58-fold, increase in SCD-2 expression in these livers. The mRNA levels of enzymes that produce NADPH, malic enzyme, glucose-6-phosphate dehydrogenase, and 6-phosphogluconate dehydrogenase, were also significantly increased (2.6 to 7-fold).

Genes involved in hepatic lipogenesis are transcriptionally regulated by sterol response element-binding protein-1c (SREBP-1c) (Horton, 2002), carbohydrate response element binding protein (ChREBP) (Uyeda and Repa, 2006), and liver X receptor (LXR) α (Joseph et al., 2002). Interestingly, in the *Agpat2*$^{-/-}$ mice, the hepatic levels of SREBP-1c mRNA were slightly increased only in males (Table 2), and more importantly, the transcriptionally active nuclear form of the SREBP-1 protein was not increased in either sex (Figure 3A). On the other hand, although the mRNA levels for ChREBP were reduced in livers of *Agpat2*$^{-/-}$ mice (0.6 to 0.7-fold) as was the total amount of nuclear protein (Figure 3A), the mRNA of the specific ChREBP target gene, L-pyruvate kinase (L-PK), was increased (~3-fold). Finally, the mRNA levels of LXR α and β were not changed and the expression of classical LXR target genes were either not changed or slightly decreased in *Agpat2*$^{-/-}$ livers (Table 2).

Peroxisome proliferator-activated receptor (PPAR) γ, another transcription factor implicated in lipogenesis, was increased by 3.1 and 1.5-fold in the males and female *Agpat2*$^{-/-}$ mice, respectively, however, its transcriptional activation is a ubiquitous feature of all steatotic livers (Browning and Horton, 2004).

To determine whether the increases in hepatic mRNA levels of lipogenic genes observed in *Agpat2*$^{-/-}$ mice reflected increased flux through the lipogenic pathway, we first measured the protein levels of ACC-1 and FAS by immunoblot analysis. As shown in the Figure 3B, the amount of both proteins was clearly increased in the livers of *Agpat2*$^{-/-}$ mice. Next, using $[^3H]_2O$, a ~4-fold increase in *de novo* hepatic fatty acid synthesis was noted in *Agpat2*$^{-/-}$ livers and a concomitant reduction in sterol synthesis was also observed (Figure 3C). Finally, the rates of *de novo* TG synthesis in primary cultured hepatocytes isolated from *Agpat2*$^{-/-}$ mouse livers by determining incorporation of [^{14}C]-glycerol into TGs were ~3-fold higher than those measured in hepatocytes from wild-type littermates (Figure 3D). Taken together, these data suggest that elevated rates of *de novo* TG synthesis contribute to the TG accumulation in *Agpat2*$^{-/-}$ mouse liver.

Hepatic steatosis could also result from a relative reduction in VLDL secretion. To test this possibility, lipoprotein lipase activity was pharmacologically blocked with Tyloxapol and VLDL secretion rates measured *in vivo*. Following Tyloxapol injection, the *Agpat2*$^{-/-}$ mice accumulated slightly more TG in plasma, suggesting that total TG secretion from liver was not reduced in the absence of AGPAT2 (Figure S8).

Finally, given that a reduction in fatty acid oxidation might contribute to the TG accumulation in *Agpat2*$^{-/-}$ livers, we evaluated the expression of genes involved in this process. PPARα, carnitine palmitoyltransferase-1 (CPT1) and acyl-coenzyme A oxidase (ACO) mRNA levels were not changed in either sex, whereas long and medium chain acyl coenzyme A dehydrogenases (LCAD and MCAD) were slightly increased in *Agpat2*$^{-/-}$ males (Table 2). Uncoupling proteins 1 and 3 (UCP1 and 3) were undetectable but UCP2 expression was increased by 10.4 and 7.4-fold in the male and female *Agpat2*$^{-/-}$ mice, respectively; however total hepatic mitochondrial β-oxidation did not differ between *Agpat2*$^{-/-}$ and wild type mice

(Figure 3E). Combined, the results suggest that reduction in fatty acid β-oxidation did not explain the TG accumulation in *Agpat2*$^{-/-}$ mouse livers.

Phospholipids and neutral lipids levels in the liver

Since PA is the substrate for various phospholipids, such as phosphatidyl ethanolamine (PE), phosphatidyl choline (PC), and phosphatidyl serine (PS); we determined whether the hepatic concentrations of these phospholipids species were altered in the *Agpat2*$^{-/-}$ mice. As shown in Figure 4A and B, PA, PE, PC, and PS concentrations were significantly elevated in the livers of male *Agpat2*$^{-/-}$ mice only. The levels of MAG were not significantly different between the wild type and *Agpat2*$^{-/-}$ mice of either gender (Figure 4C and D), but the levels of DAG were significantly increased only in the *Agpat2*$^{-/-}$ males (Figure 4E and F).

Diet Study

To test whether dietary restriction of fat might reduce hepatic steatosis in *Agpat2*$^{-/-}$ mice, wild type and *Agpat2*$^{-/-}$ mice were fed chow (6.0% fat) or a fat-free diet (0.2% fat) for 2 wk prior to study. The fat-free diet reduced liver weight by 28% and hepatic TG content by 56% in the male *Agpat2*$^{-/-}$ mice compared to chow diet. In contrast, liver weights of wild type male mice were unchanged, but liver TG content increased ~3-fold on the fat-free diet (Table 3). Similar but less dramatic changes were found in female *Agpat2*$^{-/-}$ mice (Table 3). Plasma TG and FFA levels were reduced in both the genders of *Agpat2*$^{-/-}$ mice. There was a slight reduction in body weight in *Agpat2*$^{-/-}$ mice fed the fat-free diet that was not statistically significant. Interestingly, no significant changes were observed in plasma glucose or insulin levels, indicating that hepatic steatosis was at least partially independent of the hyperinsulinemic stimuli in *Agpat2*$^{-/-}$ mice (Table 3).

The gene expression profile in the livers of the *Agpat2*$^{-/-}$ mice showed that the mRNAs encoding genes involved in *de novo* fatty acid synthesis were only slightly further increased in females and were unchanged in males on the fat-free diet (Table S2), corroborating a functional dissociation between the lipogenic activity and the TG assembly in the livers of *Agpat2*$^{-/-}$ mice. Interestingly, the fat-free diet reduced the expression of MGAT1 by 50–60% in the livers of *Agpat2*$^{-/-}$ mice, but had no effect on the levels of MGAT1 in the wild type controls (Table S2).

DISCUSSION

To understand the pathophysiology of adipose tissue loss as well as its implications on metabolic regulation, several lipodystrophic mice have been generated over the past ten years (Duan et al., 2007; Moitra et al., 1998; Shimomura et al., 1998). Our mouse model of lipodystrophy is the first to be developed based upon the genetics of human CGL and, thus has direct relevance in understanding the pathophysiology of this human disease.

Targeted gene deletion of *Agpat2* in mice resulted in a complete absence of both white and brown adipose tissue, confirming the critical role of AGPAT2 in the differentiation of both types of adipocytes. In fact, deletion of other acyltransferases involved in the glycerol-3-phosphate pathway of TG synthesis, i.e., GPAT1, AGPAT6/GPAT4, DGAT1 and 2 have not resulted in severe lipodystrophy, insulin resistance or hepatic steatosis (Beigneux et al., 2006; Buhman et al., 2002; Hammond et al., 2002; Smith et al., 2000; Stone et al., 2004; Vergnes et al., 2006). Furthermore, the phenotype of *Agpat2*$^{-/-}$ mice demonstrates that other AGPAT isoforms, mainly AGPAT1 that is also highly expressed in adipose tissue and exhibits similar acyltransferase activity *in vitro*, are unable to compensate for the absence of AGPAT2.

The *Agpat2*$^{-/-}$ mice, similar to that found in patients with CGL, type 1 (Chandalia et al., 1995), developed organomegaly including hepatosplenomegaly, nephromegaly, and elongated small intestines. This phenotype might be due to a chronic activation of the insulin-like growth factor (IGF) 1 and 2 receptors (Fradkin et al., 1989) secondary to the extreme hyperinsulinemia developed by the *Agpat2*$^{-/-}$ mice. In support of this hypothesis, IGF-1 receptor mRNA levels were indeed increased in *Agpat2*$^{-/-}$ livers (Table 2).

Although not systematically studied, female patients with CGL seem to develop more severe metabolic complications compared to males (Seip and Trygstad, 1996; Van Maldergem et al., 2002). In our mouse model, however, the female *Agpat2*$^{-/-}$ mice developed less severe hepatic steatosis or hypertriglyceridemia, as compared to their male counterparts. Both genders of *Agpat2*$^{-/-}$ mice nonetheless developed diabetes, insulin resistance and hepatomegaly. The gender dimorphism may suggest the role of testosterone and estrogen in the TG biosynthesis/metabolism in the rodent liver. Mice deficient in the aromatase enzyme (*Cyp19a1*$^{-/-}$) have recently been reported to have increased hepatic steatosis which was attenuated on estrogen supplementation (Hewitt et al., 2004; Jones et al., 2000; Murata et al., 2002). Interestingly, this phenotype was observed in the male liver only. Additional comparative studies of the livers of the *Agpat2*$^{-/-}$ male and female mice will eventually reveal a role for sex steroids and their receptors in the biosynthesis of TG.

The *Agpat2*$^{-/-}$ mice developed hepatic steatosis as early as 2–3 weeks of age. Normally, nearly all TG synthesis in liver occurs via the glycerol-3-phosphate pathway, whereas the MAG pathway remains inactive. Interestingly, despite an increase in expression of AGPATs 1, 3 and 8/ALCAT1, the total AGPAT activity remained diminished in the *Agpat2*$^{-/-}$ mouse livers. In addition, a ~5-fold increase was noted in the mRNA for GPAT1, but no significant increases in the expression of DGATs were noted. Thus, it seems that compensatory increases in the other acyltransferases implicated in the glycerol-3-phosphate pathway may not have a significant role in TG synthesis (Figure 2C).

The entire *de novo* fatty acid synthetic program was activated in *Agpat2*$^{-/-}$ mouse livers (Table 2, Figure 3A and B). The elevated lipogenesis in *Agpat2*$^{-/-}$ mouse livers resembles the findings in previous hyperinsulinemic-hyperglycemic-hepatic steatosis murine lipodystrophy models (Moitra et al., 1998;Shimomura et al., 1999); however the exact mechanism underlying the transcriptional activation of the lipogenic genes in *Agpat2*$^{-/-}$ livers remains unclear since neither SREBP-1c mRNA nor nuclear protein was elevated as has been previously demonstrated (Moitra et al., 1998;Shimomura et al., 1999) (Table 2,Figure 3A). Furthermore, the amount of nuclear ChREBP was reduced in *Agpat2*$^{-/-}$ mouse livers (Figure 3A); however, the mRNA level of L-PK, a ChREBP-regulated gene, was increased. Therefore, a potential role of ChREBP in activating lipogenesis can not be completely excluded since the transcriptional activity of ChREBP is also regulated by phosphorylation (Uyeda and Repa, 2006). Finally, it is also possible that the ~2-fold increase in PPARγ mRNA (Table 2), contributes to the activation of lipogenesis in *Agpat2*$^{-/-}$ mouse livers, but whether this is the only mechanism will require further study.

MGAT1 is reportedly expressed in the stomach, kidney, adipose tissue and, at low levels in the liver. On the other hand, MGAT2 is predominantly expressed in the small intestine (Cao et al., 2004; Cao et al., 2003; Yen and Farese, 2003; Yen et al., 2002). In our studies, MGAT1 mRNA levels were very low in the livers of wild type mice (Ct value >30); however the deletion of *Agpat2* was associated with a robust 25 to 48-fold induction of MGAT1 mRNA (Table 2) and ~5 to 7-fold increase in MGAT1 hepatic protein (Figure 2D), suggesting that enhanced TG synthesis can occur via this alternate MAG pathway in the livers of *Agpat2*$^{-/-}$ mice, such as we previously proposed (Agarwal and Garg, 2003). Unfortunately, our attempts to measure MGAT activity in the liver homogenates, which consists of mitochondria, microsomes and

cytosol, as well as in isolated microsomal preparation, using an *in vitro* assay failed most likely due to abundant activity of lipases.

The reduction in total AGPAT activity observed in *Agpat2*$^{-/-}$ livers (Figure 1B) may result in accumulation of LPA. This phospholipid can subsequently be converted into MAG by dephosphorylation mediated by type 2 PAPs. Indeed, the mRNA of type 2 PAPs known to dephosphorylate LPA, such as LPP1, isoform 1 and LPP2 were upregulated in the liver of *Agpat2*$^{-/-}$ mice (Table 2). Although lipin 3 was also upregulated, it has not been shown to have phosphatase activity against LPA (Donkor et al., 2007). The PAPs localize to plasma membrane and endoplasmic reticulum and perhaps nucleus (Carman and Han, 2008; Sigal et al., 2005). However, how increased expression of some of these phosphatases will influence conversion of LPA to MAG requires further study. Overall, these data suggest that the alternate MAG pathway is activated in the liver of *Agpat2*$^{-/-}$ mice and that it could be a mechanism for TG accumulation in these animals (Figure 2C).

Elevated concentrations of PC, PE and PS in the liver of male *Agpat2*$^{-/-}$ mice may also be explained by increased biosynthesis of DAG through the MAG pathway. In the female *Agpat2*$^{-/-}$ mice, the increases in PC, PE and PS were not statistically significant. Male *Agpat2*$^{-/-}$ mice also had higher hepatic levels of DAG compared to the wild type male mice. It is possible that increased PA levels may be related to conversion of some DAG to PA by DAG kinase. The siRNA-mediated knock down of AGPAT2 in TG-depleted cultured adipocytes increased the levels of several phospholipids and prevented adipocyte differentiation (Gale et al, 2006); however the molecular mechanism underlying this phenomenon remains unknown. It will be interesting to determine how the higher levels of PE, PC and PS contribute to the increased TG retention in the hepatocytes.

Feeding a fat-free diet resulted in a ~50% reduction in the liver TG concentration in *Agpat2*$^{-/-}$ mice (Table 3). This finding suggested that a significant proportion of the hepatic pool of TG comes from diet as chylomicrons remnants and that the increased *de novo* lipogenesis measured in *Agpat2*$^{-/-}$ mice on chow is at least partially uncoupled from TG synthesis when the mice are fed a fat-free diet, since lipogenic gene expression is still elevated (Table S2). In contrast, wild type mice accumulated hepatic TG when fed the fat-free diet. most likely due to the high carbohydrate intake, which induces *de novo* lipogenesis through the activation of SREBP-1c and ChREBP (data not shown). In normal mice, the resulting increased fatty acid synthesis is normally coupled to TG synthesis, which leads to the increase in TG accumulation.

Agpat2$^{-/-}$ mice developed a severe whole body insulin resistance and reduced expression of IR, IRS-1 and IRS-2 might be responsible for hepatic insulin resistance in the *Agpat2*$^{-/-}$ mice; a finding that is consistent with previous observations (Shimomura et al., 2000), The observed islet hypertrophy is likely a compensatory phenomenon in response to severe insulin resistance. Interestingly, severe insulin resistance was present despite normal or low levels of serum FFAs, in contrast to normal or high serum FFA levels in all other mouse models of lipodystrophy associated with hepatic steatosis (Moitra et al., 1998; Shimomura et al., 1998). This finding challenges the notion that high serum FFA levels are required to induce hepatic or peripheral insulin resistance. Thus, lipodystrophy in *Agpat2*$^{-/-}$ mice may induce hepatic steatosis and insulin resistance by diverting dietary TG for deposition in the liver. In fact, other mechanisms such as intrahepatic or intramyocellular accumulation of TGs or other intermediates in the TG biosynthetic or oxidation pathway such as DAG or ceramides may also be important (Holland et al., 2007; Nagle et al., 2007; Unger, 2003), however, we observed only a mild increase in the DAG content in the livers of male, but not female, *Agpat2*$^{-/-}$ mice.

Finally, the profound hypoleptinemia observed in *Agpat2*$^{-/-}$ mice can explain both the sustained hyperphagia and the reduced locomotor activity observed in these animals (Mesaros et al., 2008). The analysis of the RER revealed that the lipodystrophic mice rely more on oxidation of fat as an energy source and that they manifest a relative inability to utilize carbohydrates as the primary energy substrate in the fed state. This observation is consistent with whole body insulin resistance and the resulting inability of tissues to take up glucose. The hyperphagia may also be further exaggerated by the complete loss of adipose tissue, which contributes to excessive loss of heat in the lipodystrophic mice. These observations also suggest that the human infants with CGL, type 1 may also lack brown adipose tissue and thus the ability to regulate body temperature when required. The striking increase in UCP2 mRNA levels in the liver suggests that some compensatory thermogenesis is occurring there, which could be secondary to increased reactive oxygen species due to increased mitochondrial fatty acid oxidation.

In summary, *Agpat2*$^{-/-}$ mice replicate the phenotype of CGL in humans and thus, represent a unique *in vivo* model that may be exploited in future studies to elucidate the biochemical link between the TG synthesis pathway and adipogenesis in the liver and adipose tissue. Our data provide evidence for the potential role of activation of the novel alternative MAG pathway for hepatic TG biosynthesis in causing hepatic steatosis in these mice. Furthermore, we show that reduction in dietary fat mitigates hepatic steatosis in *Agpat2*$^{-/-}$ mice suggesting that dietary fat contributes significantly to hepatic accumulation of TGs.

EXPERIMENTAL PROCEDURES

Agpat2 Deletion Strategy

Details of targeting vector construction, ES culture and *Agpat2*$^{-/-}$ mice generation and genotyping are in the supplemental Experimental Procedures.

Biochemical Measurements

Plasma concentrations of TGs, insulin, glucose, free fatty acids, and liver TGs were measured as previously described (Engelking et al., 2004; Ishibashi et al., 1993; Matsuda et al., 2001).

Antibodies and Immunoblot Analysis

Rabbit polyclonal antibodies against mouse FAS and ACC1 were obtained from Genepia (Seoul, South Korea) and against SREBP-1 and SREBP-2 were prepared as previously described (Shimano et al., 1996; Shimano et al., 1997). Rabbit polyclonal antibodies against ChREBP, insulin receptor, IRS-1, IRS-2 and MGAT1 (M-90) were obtained from Novus Biologicals (Littleton, CO), BD Transduction Laboratories (San Jose, CA), Upstate (Temecula, CA) and Santa Cruz Biotechnology (Santa Cruz, CA), respectively. Details of immunoblots are presented in the supplemental Experimental Procedures section.

Real-time Reverse Transcriptase-PCR (RT-PCR)

Total RNA was prepared from mouse livers using RNA STAT-60 (Tel-Test Inc., Friendswood, TX). All RT-PCR were carried out in 384-well plates using the ABI PRISM 7900HT Sequence Detection System (Applied Biosystems) as reported previously (Liang et al., 2002; Yang et al., 2001). Primers used for additional genes are listed in Table S3.

Metabolic Rate Measurements

Indirect calorimetry, heat production, and movement were measured in 12-wk-old six wild-type female mice and five *Agpat2*$^{-/-}$ female mice using Comprehensive Lab Animal Monitoring System (CLAMS) open-circuit Oxymax system (Columbus Instruments,

Columbus, OH). Mice were individually housed in plexiglass cages through which air of known O_2 concentration was passed at a constant flow rate. After a 48-h acclimation period, exhaust air was sampled intermittently for 72 h for the determination of O_2 and CO_2. Mice were fed ad lib and all measurements were adjusted by the calculated lean mass.

In Vivo Fatty Acid and Sterols Synthesis

Hepatic fatty acids and sterols synthesis was measured in 12-wk-old, ad lib fed littermates (10 wild type, 8 *Agpat2*$^{-/-}$) by administering 50 mCi [^{3}H]$_2$O intraperitoneally as previously described (Shimano et al., 1996).

TG Synthesis Rates in Cultured Hepatocytes

TG synthesis rate was measured by incubating primary hepatocytes isolated from nonfasted wild-type (n=4) or *Agpat2*$^{-/-}$ (n=4) mice (Horton et al., 1999) with [^{14}C]-glycerol. Details are in the supplementary Experimental Procedures.

β-oxidation in Liver Mitochondria

Mitochondria were isolated from the livers of 5 to 8 wk old male and female wild type (WT) and *Agpat2*$^{-/-}$ mice. Oxidation of [^{14}C]oleate was measured as conversion to acid soluble products as described previously (McGarry et al., 1978).

AGPAT Activity in Liver Homogenates

Total AGPAT enzymatic activity was determined as described previously (Haque et al., 2005). Details are in the supplementary Experimental Procedures.

Neutral Lipids and Phospholipids in Liver Homogenates

Total lipids from the liver (~ 0.18 g wet weight) were essentially extracted as described earlier (Markham et al., 2006). The details of measurement of neutral lipids and phospholipids are provided in the Supplemental Experimental Procedures.

Statistical Analysis

For experiments comparing genotype and sex on a chow diet, two-way analysis of variance (ANOVA) was performed. To compare genotype, sex, and the regular chow versus fat free diets, three-way analysis of variance was performed. Since most of the variables were skewed and heterogeneity of variances was observed, the data were rank transformed prior to analysis. Adjustments for multiple comparisons were made using the adjust=simulate option of the GLM procedure in SAS. Statistical analysis was performed using SAS version 9.1.3 (SAS Institute, Cary, NC).

Supplementary Material

Refer to Web version on PubMed Central for supplementary material.

Acknowledgements

We thank Norma Anderson, Scott Clark, Ruth Giselle, Lauren Koob, Daniel Smith, and Judy Sanchez for technical assistance and Beverley Adams-Huet for statistical analysis. This work was supported by the National Institutes of Health grants R01-DK54387, HL20948, PL1 DK081182, HL092550, the Southwestern Medical Foundation, and the Perot Family Foundation. V.A.C. is supported by a postdoctoral fellowship from Pontificia Universidad Católica de Chile and a Presidential Fellowship from the Government of Chile. D.E.C. was supported by the UT Southwestern Physician Scientist Training Program.

References

Agarwal AK, Arioglu E, de Almeida S, Akkoc N, Taylor SI, Bowcock AM, Barnes RI, Garg A. *AGPAT2* is mutated in congenital generalized lipodystrophy linked to chromosome 9q34. Nat Genet 2002;31:21–23. [PubMed: 11967537]

Agarwal AK, Barnes RI, Garg A. Functional characterization of human 1-acylglycerol-3-phosphate acyltransferase isoform 8: cloning, tissue distribution, gene structure and enzymatic activity. Arch Biochem Biophys 2006;449:64–76. [PubMed: 16620771]

Agarwal AK, Garg A. Congenital generalized lipodystrophy: significance of triglyceride biosynthetic pathways. Trends Endocrinol Metab 2003;14:214–221. [PubMed: 12826327]

Agarwal AK, Garg A. Genetic disorders of adipose tissue development, differentiation, and death. Annu Rev Genomics Hum Genet 2006;7:175–199. [PubMed: 16722806]

Agarwal AK, Simha V, Oral EA, Moran SA, Gorden P, O'Rahilly S, Zaidi Z, Gurakan F, Arslanian SA, Klar A, Ricker A, White NHLB, Herbst K, Kennel K, Patel SB, Al-Gazali L, Garg A. Phenotypic and genetic heterogeneity in congenital generalized lipodystrophy. J Clin Endocrinol Metab 2003;88:4840–4847. [PubMed: 14557463]

Agarwal AK, Sukumaran S, Bartz R, Barnes RI, Garg A. Functional characterization of human 1-acylglycerol-3-phosphate-O-acyltransferase isoform 9: cloning, tissue distribution, gene structure, and enzymatic activity. J Endocrinol 2007;193:445–457. [PubMed: 17535882]

Beigneux AP, Vergnes L, Qiao X, Quatela S, Davis R, Watkins SM, Coleman RA, Walzem RL, Philips M, Reue K, Young SG. Agpat6-a novel lipid biosynthetic gene required for triacylglycerol production in mammary epithelium. J Lipid Res 2006;47:734–744. [PubMed: 16449762]

Brindley DN. Lipid phosphate phosphatases and related proteins: signaling functions in development, cell division, and cancer. J Cell Biochem 2004;92:900–912. [PubMed: 15258914]

Brindley DN, Waggoner DW. Mammalian lipid phosphate phosphohydrolases. J Biol Chem 1998;273:24281–24284. [PubMed: 9733709]

Browning JD, Horton JD. Molecular mediators of hepatic steatosis and liver injury. J Clin Invest 2004;114:147–152. [PubMed: 15254578]

Buhman KK, Smith SJ, Stone SJ, Repa JJ, Wong JS, Knapp FF Jr, Burri BJ, Hamilton RL, Abumrad NA, Farese RV Jr. DGAT1 is not essential for intestinal triacylglycerol absorption or chylomicron synthesis. J Biol Chem 2002;277:25474–25479. [PubMed: 11959864]

Cao J, Hawkins E, Brozinick J, Liu X, Zhang H, Burn P, Shi Y. A predominant role of acyl-CoA: monoacylglycerol acyltransferase-2 in dietary fat absorption implicated by tissue distribution, subcellular localization, and up-regulation by high fat diet. J Biol Chem 2004;279:18878–18886. [PubMed: 14966132]

Cao J, Li JL, Li D, Tobin JF, Gimeno RE. Molecular identification of microsomal acyl-CoA:glycerol-3-phosphate acyltransferase, a key enzyme in de novo triacylglycerol synthesis. Proc Natl Acad Sci U S A 2006;103:19695–19700. [PubMed: 17170135]

Cao J, Lockwood J, Burn P, Shi Y. Cloning and functional characterization of a mouse intestinal acyl-CoA: monoacylglycerol acyltransferase, MGAT2. J Biol Chem 2003;278:13860–13866. [PubMed: 12576479]

Carman GM, Han GS. Roles of phosphatidate phosphatase enzymes in lipid metabolism. Trends Biochem Sci 2006;31:694–699. [PubMed: 17079146]

Carman GM, Han GS. Phosphatidic acid phosphatase, a key enzyme in the regulation of lipid synthesis. J Biol Chem. 2008

Chandalia M, Garg A, Vuitch F, Nizzi F. Postmortem findings in congenital generalized lipodystrophy. J Clin Endocrinol Metab 1995;80:3077–3081. [PubMed: 7559900]

Chen YQ, Kuo MS, Li S, Bui HH, Peake DA, Sanders PE, Thibodeaux SJ, Chu S, Qian YW, Zhao Y, Bredt DS, Moller DE, Konrad RJ, Beigneux AP, Young SG, Cao G. AGPAT6 is a novel microsomal glycerol-3-phosphate acyltransferase. J Biol Chem 2008;283:10048–10057. [PubMed: 18238778]

Donkor J, Sariahmetoglu M, Dewald J, Brindley DN, Reue K. Three mammalian lipins act as phosphatidate phosphatases with distinct tissue expression patterns. J Biol Chem 2007;282:3450–3457. [PubMed: 17158099]

Duan SZ, Ivashchenko CY, Whitesall SE, D'Alecy LG, Duquaine DC, Brosius FC, Gonzalez FJ, Vinson C, Pierre MA, Milstone DS, Mortensen RM. Hypotension, lipodystrophy, and insulin resistance in generalized PPARgamma-deficient mice rescued from embryonic lethality. J Clin Invest 2007;117:812–822. [PubMed: 17304352]

Engelking LJ, Kuriyama H, Hammer RE, Horton JD, Brown MS, Goldstein JL, Liang G. Overexpression of Insig-1 in the livers of transgenic mice inhibits SREBP processing and reduces insulin-stimulated lipogenesis. J Clin Invest 2004;113:1168–1175. [PubMed: 15085196]

Fradkin JE, Eastman RC, Lesniak MA, Roth J. Specificity spillover at the hormone receptor--exploring its role in human disease. N Engl J Med 1989;320:640–645. [PubMed: 2537464]

Gale SE, Frolov A, Han X, Bickel PE, Cao L, Bowcock A, Schaffer JE, Ory DS. A regulatory role for 1-acylglycerol-3-phosphate-O-acyltransferase 2 in adipocyte differentiation. J Biol Chem 2006;281:11082–11089. [PubMed: 16495223]

Garg A. Acquired and genetic lipodystrophies. N Engl J Med 2004;350:1220–1234. [PubMed: 15028826]

Hammond LE, Gallagher PA, Wang S, Hiller S, Kluckman KD, Posey-Marcos EL, Maeda N, Coleman RA. Mitochondrial glycerol-3-phosphate acyltransferase-deficient mice have reduced weight and liver triacylglycerol content and altered glycerolipid fatty acid composition. Mol Cell Biol 2002;22:8204–8214. [PubMed: 12417724]

Haque W, Garg A, Agarwal AK. Enzymatic activity of naturally occurring 1-acylglycerol-3-phosphate-O-acyltransferase 2 mutants associated with congenital generalized lipodystrophy. Biochem Biophys Res Commun 2005;327:446–453. [PubMed: 15629135]

Hewitt KN, Pratis K, Jones ME, Simpson ER. Estrogen replacement reverses the hepatic steatosis phenotype in the male aromatase knockout mouse. Endocrinology 2004;145:1842–1848. [PubMed: 14684602]

Holland WL, Brozinick JT, Wang LP, Hawkins ED, Sargent KM, Liu Y, Narra K, Hoehn KL, Knotts TA, Siesky A, Nelson DH, Karathanasis SK, Fontenot GK, Birnbaum MJ, Summers SA. Inhibition of ceramide synthesis ameliorates glucocorticoid-, saturated-fat-, and obesity-induced insulin resistance. Cell Metab 2007;5:167–179. [PubMed: 17339025]

Horton JD. Sterol regulatory element-binding proteins: transcriptional activators of lipid synthesis. Biochem Soc Trans 2002;30:1091–1095. [PubMed: 12440980]

Horton JD, Shimano H, Hamilton RL, Brown MS, Goldstein JL. Disruption of LDL receptor gene in transgenic SREBP-1a mice unmasks hyperlipidemia resulting from production of lipid-rich VLDL. J Clin Invest 1999;103:1067–1076. [PubMed: 10194480]

Ishibashi S, Brown MS, Goldstein JL, Gerard RD, Hammer RE, Herz J. Hypercholesterolemia in low density lipoprotein receptor knockout mice and its reversal by adenovirus-mediated gene delivery. J Clin Invest 1993;92:883–893. [PubMed: 8349823]

Jones ME, Thorburn AW, Britt KL, Hewitt KN, Wreford NG, Proietto J, Oz OK, Leury BJ, Robertson KM, Yao S, Simpson ER. Aromatase-deficient (ArKO) mice have a phenotype of increased adiposity. Proc Natl Acad Sci U S A 2000;97:12735–12740. [PubMed: 11070087]

Joseph SB, Laffitte BA, Patel PH, Watson MA, Matsukuma KE, Walczak R, Collins JL, Osborne TF, Tontonoz P. Direct and indirect mechanisms for regulation of fatty acid synthase gene expression by liver X receptors. J Biol Chem 2002;277:11019–11025. [PubMed: 11790787]

Leung DW. The structure and functions of human lysophosphatidic acid acyltransferases. Front Biosci 2001;6:d944–953. [PubMed: 11487472]

Li D, Yu L, Wu H, Shan Y, Guo J, Dang Y, Wei Y, Zhao S. Cloning and identification of the human LPAAT-zeta gene, a novel member of the lysophosphatidic acid acyltransferase family. J Hum Genet 2003;48:438–442. [PubMed: 12938015]

Liang G, Yang J, Horton JD, Hammer RE, Goldstein JL, Brown MS. Diminished hepatic response to fasting/refeeding and liver X receptor agonists in mice with selective deficiency of sterol regulatory element-binding protein-1c. J Biol Chem 2002;277:9520–9528. [PubMed: 11782483]

Markham JE, Li J, Cahoon EB, Jaworski JG. Separation and identification of major plant sphingolipid classes from leaves. J Biol Chem 2006;281:22684–22694. [PubMed: 16772288]

Matsuda M, Korn BS, Hammer RE, Moon YA, Komuro R, Horton JD, Goldstein JL, Brown MS, Shimomura I. SREBP cleavage-activating protein (SCAP) is required for increased lipid synthesis

in liver induced by cholesterol deprivation and insulin elevation. Genes Dev 2001;15:1206–1216. [PubMed: 11358865]

McGarry JD, Mannaerts GP, Foster DW. Characteristics of fatty acid oxidation in rat liver homogenates and the inhibitory effect of malonyl-CoA. Biochim Biophys Acta 1978;530:305–313. [PubMed: 698234]

Mesaros A, Koralov SB, Rother E, Wunderlich FT, Ernst MB, Barsh GS, Rajewsky K, Bruning JC. Activation of Stat3 signaling in AgRP neurons promotes locomotor activity. Cell Metab 2008;7:236–248. [PubMed: 18316029]

Moitra J, Mason MM, Olive M, Krylov D, Gavrilova O, Marcus-Samuels B, Feigenbaum L, Lee E, Aoyama T, Eckhaus M, Reitman ML, Vinson C. Life without white fat: a transgenic mouse. Genes Dev 1998;12:3168–3181. [PubMed: 9784492]

Murata Y, Robertson KM, Jones ME, Simpson ER. Effect of estrogen deficiency in the male: the ArKO mouse model. Mol Cell Endocrinol 2002;193:7–12. [PubMed: 12160996]

Nagle CA, An J, Shiota M, Torres TP, Cline GW, Liu ZX, Wang S, Catlin RL, Shulman GI, Newgard CB, Coleman RA. Hepatic overexpression of glycerol-sn-3-phosphate acyltransferase 1 in rats causes insulin resistance. J Biol Chem 2007;282:14807–14815. [PubMed: 17389595]

Seip M, Trygstad O. Generalized lipodystrophy, congenital and acquired (lipoatrophy). Acta Paediatrica Supplement 1996;413:2–28. [PubMed: 8783769]

Shimano H, Horton JD, Hammer RE, Shimomura I, Brown MS, Goldstein JL. Overproduction of Cholesterol and Fatty Acids Causes Massive Liver Enlargement in Transgenic Mice Expressing Truncated Srebp-1a. J Clin Invest 1996;98:1575–1584. [PubMed: 8833906]

Shimano H, Horton JD, Shimomura I, Hammer RE, Brown MS, Goldstein JL. Isoform 1c of Sterol Regulatory Element Binding Protein Is Less Active Than Isoform 1a in Livers of Transgenic Mice and in Cultured Cells. J Clin Invest 1997;99:846–854. [PubMed: 9062341]

Shimomura I, Bashmakov Y, Horton JD. Increased levels of nuclear SREBP-1c associated with fatty livers in two mouse models of diabetes mellitus. J Biol Chem 1999;274:30028–30032. [PubMed: 10514488]

Shimomura I, Hammer RE, Richardson JA, Ikemoto S, Bashmakov Y, Goldstein JL, Brown MS. Insulin resistance and diabetes mellitus in transgenic mice expressing nuclear SREBP-1c in adipose tissue: model for congenital generalized lipodystrophy. Genes Dev 1998;12:3182–3194. [PubMed: 9784493]

Shimomura I, Matsuda M, Hammer RE, Bashmakov Y, Brown MS, Goldstein JL. Decreased IRS-2 and increased SREBP-1c lead to mixed insulin resistance and sensitivity in livers of lipodystrophic and ob/ob mice. Molecular Cell 2000;6:77–86. [PubMed: 10949029]

Sigal YJ, McDermott MI, Morris AJ. Integral membrane lipid phosphatases/phosphotransferases: common structure and diverse functions. Biochem J 2005;387:281–293. [PubMed: 15801912]

Smith SJ, Cases S, Jensen DR, Chen HC, Sande E, Tow B, Sanan DA, Raber J, Eckel RH, Farese RV Jr. Obesity resistance and multiple mechanisms of triglyceride synthesis in mice lacking Dgat. Nat Genet 2000;25:87–90. [PubMed: 10802663]

Stone SJ, Myers HM, Watkins SM, Brown BE, Feingold KR, Elias PM, Farese RV Jr. Lipopenia and skin barrier abnormalities in DGAT2-deficient mice. J Biol Chem 2004;279:11767–11776. [PubMed: 14668353]

Tang W, Yuan J, Chen X, Gu X, Luo K, Li J, Wan B, Wang Y, Yu L. Identification of a novel human lysophosphatidic acid acyltransferase, LPAAT-theta, which activates mTOR pathway. Journal of biochemistry and molecular biology 2006;39:626–635. [PubMed: 17002884]

Unger RH. Lipid overload and overflow: metabolic trauma and the metabolic syndrome. Trends Endocrinol Metab 2003;14:398–403. [PubMed: 14580758]

Uyeda K, Repa JJ. Carbohydrate response element binding protein, ChREBP, a transcription factor coupling hepatic glucose utilization and lipid synthesis. Cell Metab 2006;4:107–110. [PubMed: 16890538]

Van Maldergem L, Magre J, Khallouf TE, Gedde-Dahl T Jr, Delepine M, Trygstad O, Seemanova E, Stephenson T, Albott CS, Bonnici F, Panz VR, Medina JL, Bogalho P, Huet F, Savasta S, Verloes A, Robert JJ, Loret H, De Kerdanet M, Tubiana-Rufi N, Megarbane A, Maassen J, Polak M, Lacombe D, Kahn CR, Silveira EL, D'Abronzo FH, Grigorescu F, Lathrop M, Capeau J, O'Rahilly S.

Genotype-phenotype relationships in Berardinelli-Seip congenital lipodystrophy. J Med Genet 2002;39:722–733. [PubMed: 12362029]

Vergnes L, Beigneux AP, Davis R, Watkins SM, Young SG, Reue K. Agpat6 deficiency causes subdermal lipodystrophy and resistance to obesity. J Lipid Res 2006;47:745–754. [PubMed: 16436371]

West J, Tompkins CK, Balantac N, Nudelman E, Meengs B, White T, Bursten S, Coleman J, Kumar A, Singer JW, Leung DW. Cloning and expression of two human lysophosphatidic acid acyltransferase cDNAs that enhance cytokine-induced signaling responses in cells. DNA Cell Biol 1997;16:691–701. [PubMed: 9212163]

Yang J, Goldstein JL, Hammer RE, Moon YA, Brown MS, Horton JD. Decreased lipid synthesis in livers of mice with disrupted Site-1 protease gene. Proc Natl Acad Sci USA 2001;98:13607–13612. [PubMed: 11717426]

Ye GM, Chen C, Huang S, Han DD, Guo JH, Wan B, Yu L. Cloning and characterization a novel human 1-acyl-sn-glycerol-3-phosphate acyltransferase gene AGPAT7. DNA Seq 2005;16:386–390. [PubMed: 16243729]

Yen CL, Farese RV Jr. MGAT2, a monoacylglycerol acyltransferase expressed in the small intestine. J Biol Chem 2003;278:18532–18537. [PubMed: 12621063]

Yen CL, Stone SJ, Cases S, Zhou P, Farese RV Jr. Identification of a gene encoding MGAT1, a monoacylglycerol acyltransferase. Proc Natl Acad Sci U S A 2002;99:8512–8517. [PubMed: 12077311]

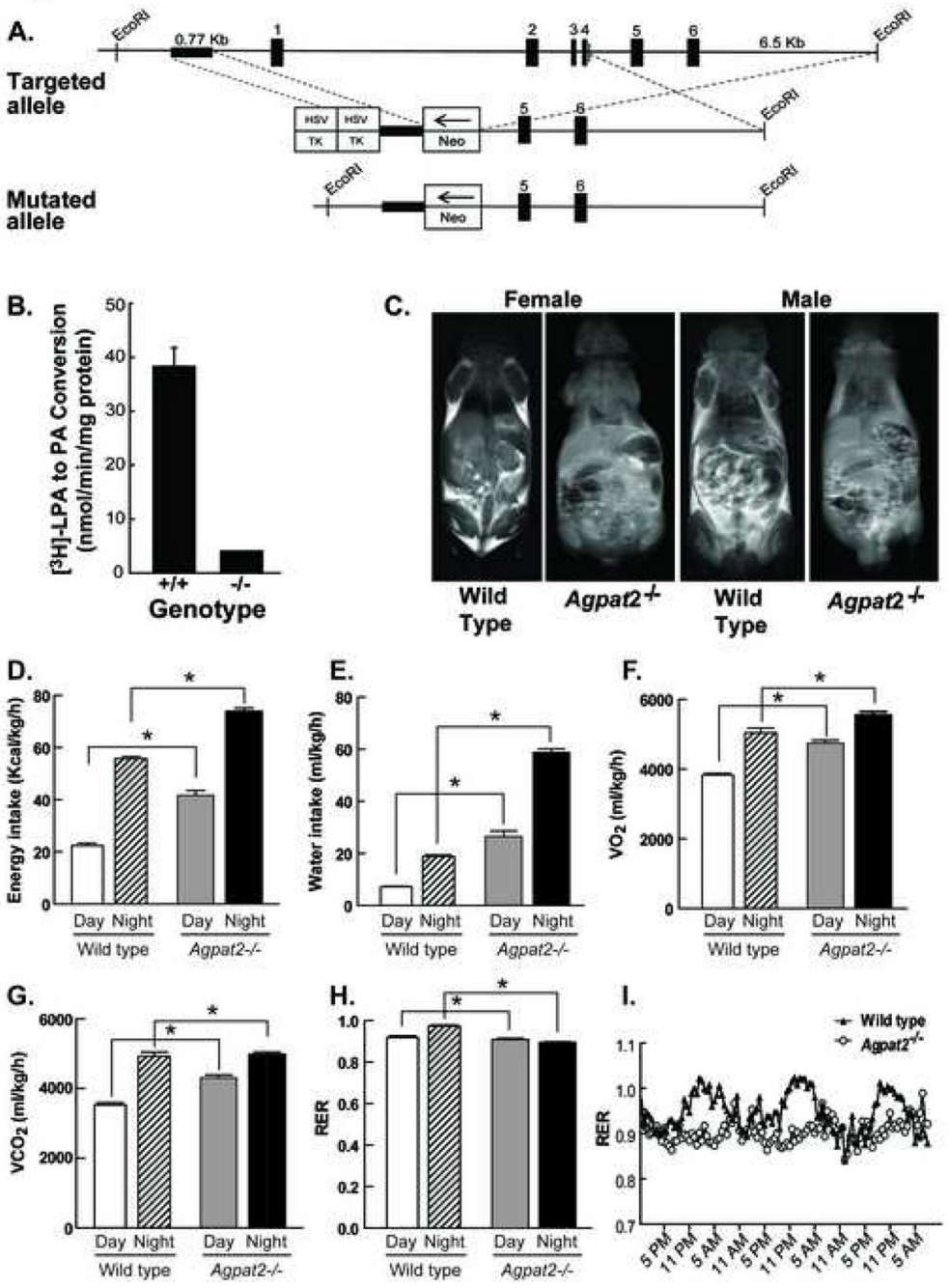

Figure 1. Strategy to disrupt *Agpat2* in mice. *Agpat2*$^{-/-}$ mice have markedly reduced total hepatic AGPAT activity, complete lack of adipose tissue and abnormal energy metabolism

(A) The map of the wild type allele is shown for exons 1–6 of *Agpat2*. The genomic sequence spanning a portion of the promoter and exons 1–4 were replaced with the neomycin-resistance cassette (NEO). Abbreviation: Herpes simplex virus thymidine kinase, HSC-TK

(B) Total AGPAT activity in the liver homogenates of the *Agpat2*$^{-/-}$ mice revealed significantly reduced activity (10% of that measured in wild type mouse livers). Livers from 6 *Agpat2*$^{-/-}$ mice and 6 wild type mice were studied.

(C) Magnetic resonance imaging of the male and female wild type and *Agpat2*$^{-/-}$ mice. Coronal sections were obtained on the whole body mid-section for 3 males and 3 females *Agpat2*$^{-/-}$

and 3 male and 3 female wild type mice. The wild type mice show adipose tissue in the subcutaneous and intra-abdominal regions as areas of increased signal intensity on T-1 weighted images. The *Agpat2*$^{-/-}$ mice in contrast have no adipose tissue.
(D) energy intake, (E) water intake, (F) O_2 consumption (G) CO_2 production, (H) Respiratory Exchange Ratio (RER) and (I) RER time course in wild type (unfilled bars and hatched bars for the day and night data, respectively) and *Agpat2*$^{-/-}$ mice (filled gray and black bars for the day and night data, respectively). The data are normalized to lean body mass, which was 5.7% greater in *Agpat2*$^{-/-}$ mice. Bars represent the mean and the whiskers represent SEM. * indicates $p<0.05$ in the comparison between the two genotypes for the same period (day or night).

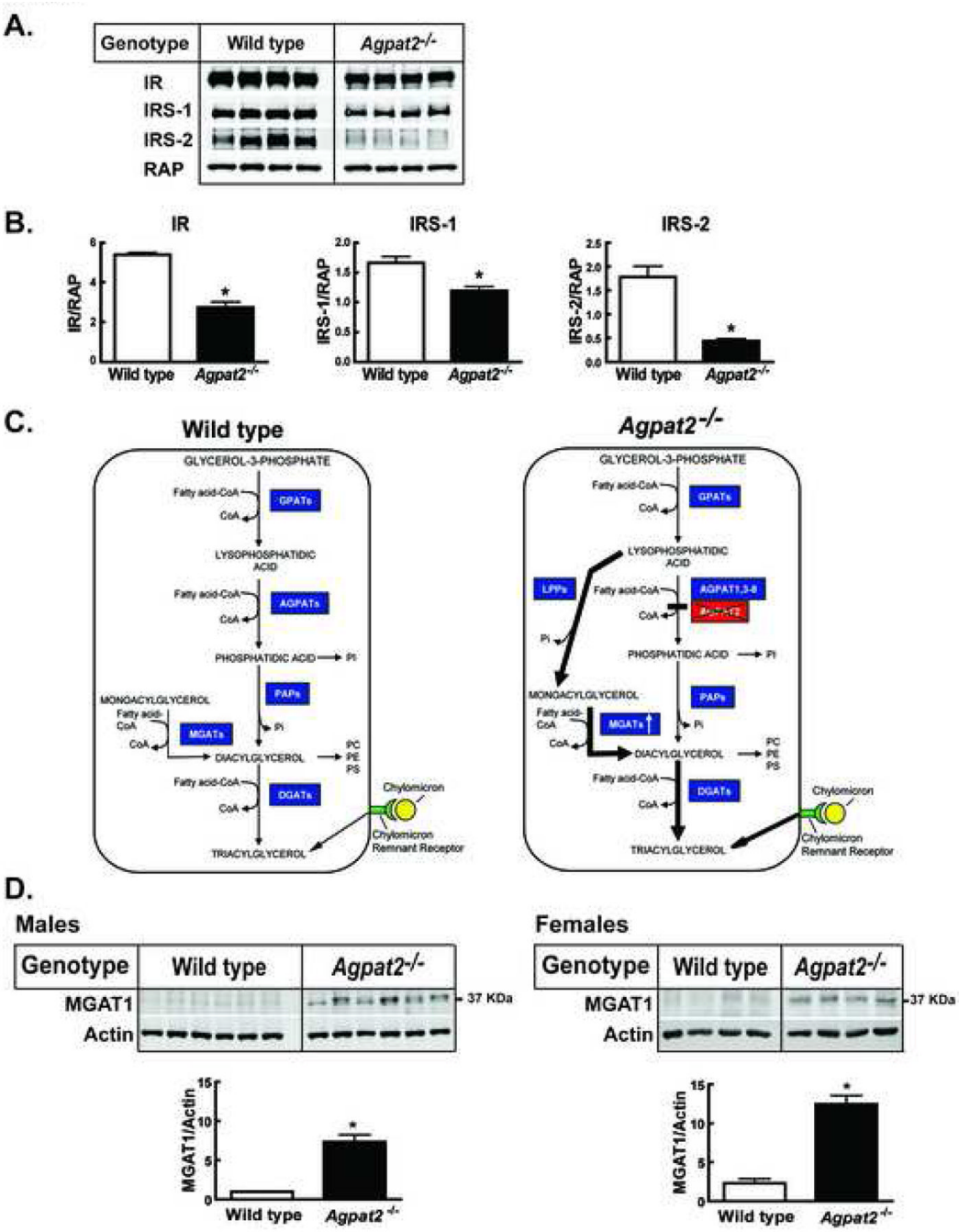

Figure 2. Immunoblot analysis of insulin receptor subunit β (IR), IRS-1, IRS-2 and MGAT1 and models for cellular TG biosynthetic pathways in the wild type and *Agpat2*$^{-/-}$ mice

(A) Whole cell extracts were prepared from the livers of four wild type and *Agpat2*$^{-/-}$ female mice and equal aliquots (30 μg) were individually transferred to nitrocellulose membranes, incubated with the corresponding primary and IRDye800-conjugated secondary antibodies and scanned as described in "Supplementary Experimental Procedures". Receptor associated protein (RAP) was used as the loading control.

(B) The absolute signal intensity of IR, IRS-1 and IRS-2 was normalized to the corresponding signal of RAP and the mean values of the ratios were compared. Bars represent the mean ± S.E.M. * indicates $p < 0.05$, Student's t test.

(C) Pathways for hepatic TG accumulation in the wild type and *Agpat2*$^{-/-}$ mice. The left panel shows that hepatocytes can synthesize TG from either the glycerol-3-phosphate (G-3-P) or the monoacylglycerol (MAG) pathway and accumulate TG from receptor-mediated uptake of chylomicron remnants. G-3-P is the initial substrate for acylation at the sn-1 position by G-3-P acyltransferases (GPATs), to form 1-acylglycerol-3-phosphate or lysophosphatidic acid (LPA). LPA is further acylated at the sn-2 position by 1-acylglycerol-3-phosphate acyltransferases (AGPATs) to form phosphatidic acid (PA). In the next step, the phosphate group (Pi) is removed by type 1 phosphatidate phosphohydrolases (PAPs) to produce diacylglycerol (DAG). DAG is further acylated at the sn-3 position by DAG acyltransferases (DGATs) to produce triacylglycerol (TG). In addition, TG can also be synthesized via the acylation of 1- or 2 MAG by the enzymes MAG-acyltransferases (MGATs). Normally, most of TG biosynthesis occurs via G-3-P pathway.
In *Agpat2*$^{-/-}$ mice (Right Panel), the suppression of AGPAT activity interrupts the classical G-3-P pathway which might result in accumulation of intracellular LPA. The concomitant overexpression of lipid phosphate phosphatases (LPPs) and MGAT1 observed in livers of *Agpat2*$^{-/-}$ mice could divert LPA to 1-MAG and DAG through an alternate pathway, which would allow the assembly of TGs by DGATs-mediated acylation. Additionally, the marked reduction in the hepatic steatosis observed in *Agpat2*$^{-/-}$ mice upon feeding fat-free diet suggests that dietary fat also contributes to the accumulation of TG in the liver.
(D) Total membranes were prepared from the livers of the wild type and *Agpat2*$^{-/-}$ mice described in Table 2. Individual aliquots (30 μg) of membrane proteins were transferred into nitrocellulose membranes, incubated with actin or MGAT1 primary antibodies and IRDye680 or IRDy800-conjugated secondary antibodies, and quantified as described in “Supplementary Experimental Procedures”. Each specific MGAT1 signal was normalized to the respective actin loading control and then normalized to the MGAT1/Actin average signal in male wild type mice. The mean of each group is represented ± SEM * denotes $P < 0.05$.

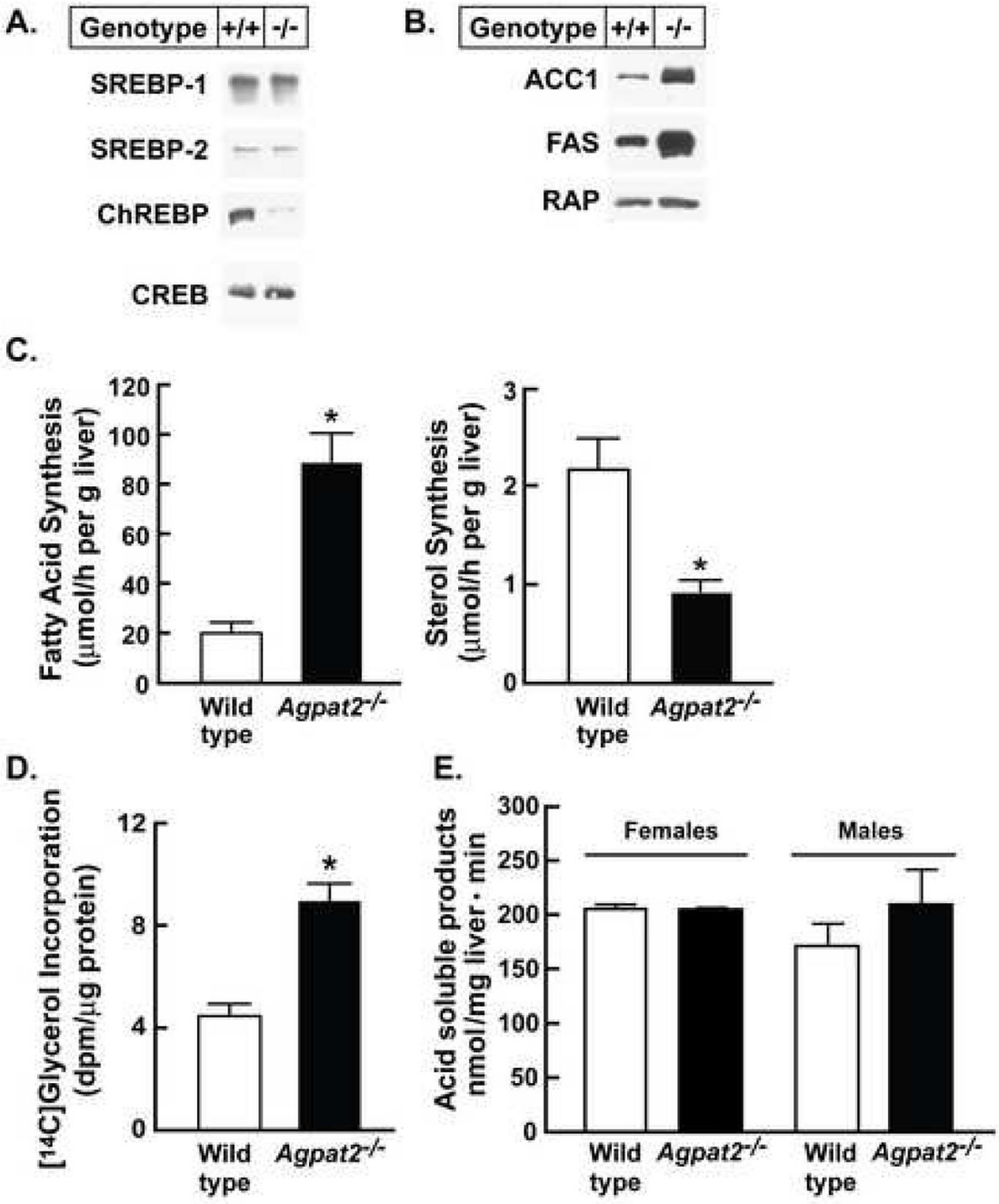

Figure 3. *Agpat2*$^{-/-}$ mice have no change in liver nuclear SREBPs and ChREBP protein and mitochondrial fatty acid oxidation but have increased levels of lipogenic proteins and rates of fatty acids and TG synthesis

(A) Immunoblot analysis of SREBP-1, SREBP-2, and ChREBP. Nuclear proteins were prepared from individual livers of 5 male wild type and *Agpat2*$^{-/-}$ mice. Equal aliquots from each liver were pooled and 20 μg of nuclear extract protein was subjected to SDS-PAGE and immunoblotting using anti-mouse SREBP-1, SREBP-2, and ChREBP antibodies. The cAMP response element-binding (CREB) protein was used as the loading control.

(B) Immunoblot analysis of ACC1 and FAS. Total cell lysate protein was isolated from individual livers of 4 male wild type and *Agpat2*$^{-/-}$ mice. Equal aliquots were pooled and 30

μg of protein was subjected to 8% SDS-PAGE for immunoblot analysis. RAP was used as a control for loading.

(C) *In vivo* rates of hepatic fatty acid and sterol synthesis in 10 wild type and 8 *Agpat2*$^{-/-}$ mice using [^{3}H]$_{2}$O. Each bar represents the mean ± SEM. * indicates $p<0.05$ between the two genotypes using Student's *t*-test.

(D) TG synthesis rates were determined in primary hepatocytes from four wild type and *Agpat2*$^{-/-}$ female mice by measuring the incorporation of [^{14}C]glycerol into newly synthesized TGs. Bars represent the mean ± SEM. * indicates $p<0.05$ between the two genotypes using Student's *t*-test.

(E) Hepatic mitochondrial β-oxidation was measured as production of acid soluble products in wild type and *Agpat2*$^{-/-}$ mice of both genders (n=4 each). Bars represent mean ± SEM.

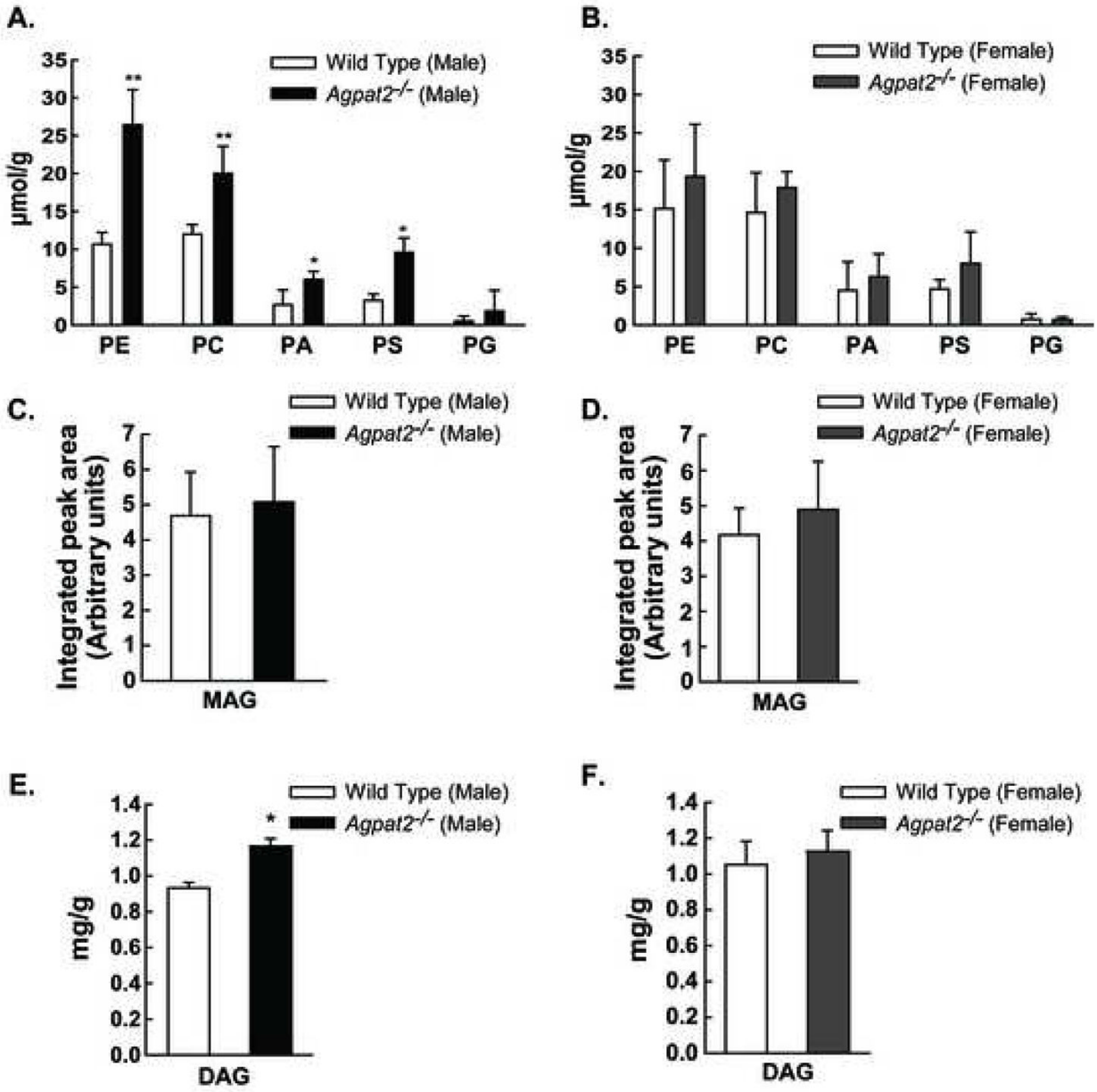

Figure 4. Sexual dimorphism in the hepatic lipid composition of *Agpat2*$^{-/-}$ mice

(A) and (B) Hepatic concentrations of phosphatidyl ethanolamine (PE), phosphatidyl choline (PC), phosphatidic acid (PA), phosphatidyl serine (PS) and phosphatidyl glycerol (PG) in mol per g of liver tissue in male and female wild type and *Agpat2*$^{-/-}$ mice.

(C)–(F) Concentrations of monoacylglycerol (MAG) and diacylglycerol (DAG) in the liver homogenates from the male and female wild type and *Agpat2*$^{-/-}$ mice. No statistically significant differences were found between the female wild type and *Agpat2*$^{-/-}$ mice among the various phospholipid, MAG, and DAG species measured. * indicates $p < 0.05$ for the comparison between the male wild type and *Agpat2*$^{-/-}$ mice.

Table 1

Phenotypic comparison of wild type and *Agpat2*$^{-/-}$ mice

Gender	**Male**		**Female**	
Genotype	**Wild type**	***Agpat2*$^{-/-}$**	**Wild type**	***Agpat2*$^{-/-}$**
Number of mice	10	10	10	10
Body weight, g	25.9 ± 2.4	24.7 ± 4.4	25.9 ± 3.6	25.6 ±3.6
Liver weight, g	1.40 ± 0.19	3.52 ± 0.67*	1.43 ± 0.29	4.1 ± 1.1*
Liver TGs, mg/g	7.5 ± 2.7	48.2 ± 17.4*	18.1 ± 9.4	37.4 ± 18.8*
Plasma TGs, mg/dL	83 ± 23	153 ± 48*	84 ± 26	105 ± 23
Plasma insulin, ng/mL	0.8 ± 0.4	49.0 ± 48.0*	0.9 ± 0.4	66.4 ± 49.7*
Plasma glucose, mg/dL	303 ± 54	428 ± 75*	286 ± 85	428 ± 113*
Plasma FFA, mEq/L	0.53 ± 0.13	0.55 ± 0.10	0.54 ± 0.18	0.37 ± 0.12*
WAT weight†, g	0.24 ± 0.01	0*	0.37 ± 0.09	0*
BAT weight†, g	0.05 ± 0.01	0*	0.08 ± 0.01	0*
Plasma Leptin†, ng/mL	2.23 ± 0.34	0.41 ± 0.05*	4.02 ± 2.13	0.21 ± 0.28*

Mice (11–15 weeks of age) were fed a standard rodent chow and killed in the non-fasted state. Each value represents the mean ± S.D.

*denotes a level of statistical significance of $P<0.05$ between the wild type and *Agpat2*$^{-/-}$ mice. Abbreviations used: WAT, epididymal and perigonadal white adipose tissue for male and female mice, respectively; BAT, brown adipose tissue; FFA, free fatty acids; TG, triglycerides.

†These observations were made in 5 animals from each group.

Table 2

Relative expression of liver mRNAs of male and female *Agpat2*$^{-/-}$ mice.

Genotype	***Agpat2*$^{-/-}$**	***Agpat2*$^{-/-}$**
Sex	**Male**	**Female**
mRNA	Fold change	Fold change
Fatty acid and TG synthesis		
ATP citrate lyase	5.1 ± 1.1*	3.1 ± 0.8*
ACC-1	5.5 ± 0.6*	3.9 ± 0.6*
FAS	9.9 ± 0.8*	4.7 ± 0.7*
ELOVL6	9.3 ± 0.8*	4.9 ± 0.6*
SCD-1	5.7 ± 0.7*	4.2 ± 0.3*
SCD-2	57.7 ± 9.4*	55.5 ± 4.1*
AGPAT1	1.7 ± 0.04*	1.2 ± 0.1
AGPAT2	0	0
AGPAT3	1.5 ± 0.1*	1.4 ± 0.1*
AGPAT4	ND	ND
AGPAT5	1.6 ± 0.1*	1.3 ± 0.1
AGPAT6/GPAT4	0.8 ± 0.05	0.9 ± 0.1
AGPAT7/LPEAT2	1.8 ± 0.2	1.6 ± 0.3
AGPAT8/ALCAT1	4.6 ± 0.9*	1.6 ± 0.1*
MGAT1	47.7 ± 7.1*	24.5 ± 2.6*
MGAT2	ND	ND
DGAT1	ND	ND
DGAT2	0.9 ± 0.01	0.7 ± 0.1
GPAT1	4.7 ± 0.5*	4.8 ± 0.9*
PPAR-γ	3.1 ± 0.1*	1.5 ± 0.1*
Phosphatidic acid phosphatase 2a-1 (LPP1)	2.0 ± 0.05*	1.5 ± 0.1*
Phosphatidic acid phosphatase 2a-2 (LPP1)	1.3 ± 0.03*	1.3 ± 0.1
Phosphatidic acid phosphatase 2b (LPP3)	1.0 ± 0.1	0.7 ± 0.0*
Phosphatidic acid phosphatase 2c (LPP2)	3.4 ± 0.3*	2.0 ± 0.1*
Lipin 1	0.8 ± 0.2	2.1 ± 0.2*
Lipin 2	1.3 ± 0.1	1.8 ± 0.1*
Lipin 3	2.6 ± 0.5*	2.1 ± 0.3*
Fatty acid oxidation		
PPAR-α	1.0 ± 0.1	1.0 ± 0.1
Carnitine palmitoyl transferase 1	1.1 ± 0.1	1.2 ± 0.1
Acyl-CoA oxidase-1	1.3 ± 0.1	1.1 ± 0.1
Long-chain acyl-CoA dehydrogenase	1.6 ± 0.1*	1.0 ± 0.1
Medium-chain acyl-CoA dehydrogenase	1.9 ± 0.2*	1.0 ± 0.1
UCP-1	ND	ND
UCP-2	10.4 ± 0.4*	7.4 ± 0.2*

Genotype	***Agpat2*$^{-/-}$**	***Agpat2*$^{-/-}$**
Sex	**Male**	**Female**
UCP-3	ND	ND
SREBP pathway		
SREBP-1a	1.3 ± 0.1*	1.2 ± 0.04
SREBP-1c	1.4 ± 0.1*	0.9 ± 0.1
SREBP-2	1.3 ± 0.1*	1.0 ± 0.1
SCAP	0.8± 0.1	0.7 ± 0.03*
Insig-1	1.4 ± 0.04*	1.4 ± 0.05
Insig-2	1.9 ± 0.1*	1.3 ± 0.3
Insulin and IGF-1 signaling		
Insulin receptor	0.9 ± 0.04	0.8 ± 0.1
Insulin receptor substrate-1	1.3 ± 0.2	0.9 ± 0.1
Insulin receptor substrate-2	0.4 ± 0.03*	0.3 ± 0.04*
IGF-1	0.2 ± 0.03*	0.1 ± 0.02*
IGF-1 receptor	1.5 ± 0.1*	2.0 ± 0.3*
IGF binding protein 1	7.2 ± 4.5	6.9 ± 1.5*
Glucose metabolism		
ChREBP	0.6 ± 0.04	0.7 ± 0.1
Phosphoenolpyruvate carboxykinase	0.6 ± 0.1*	0.6 ± 0.2
Glucokinase	2.0 ± 0.3*	2.3 ± 0.1*
Glucose-6-phosphatase	1.8 ± 0.2	3.2 ± 0.6*
L-Pyruvate kinase	3.5 ± 0.3*	3.4 ± 0.2*
NADPH-producing		
Malic enzyme	5.8 ± 0.4*	4.5 ± 0.3*
Glucose-6- phosphate dehydrogenase	2.7 ± 0.2*	2.6 ± 0.2*
6-Phosphogluconate dehydrogenase	7.0 ± 0.6*	6.1 ± 0.7*
LXRs and target genes		
LXR α	1.1 ± 0.1	1.0 ± 0.1
LXR β	1.3 ± 0.1	1.0 ± 0.1
ABCA1	1.0± 0.1	1.1 ± 0.04
ABCG5	0.8 ± 0.1	0.5 ± 0.1*
ABCG8	0.5 ± 0.1*	0.5 ± 0.04*
CYP7A1	0.6 ± 0.1	0.2 ± 0.02*

Each value represents the mean fold change (± S.E.M.) of 4 individual male or female *Agpat2*$^{-/-}$ mice in comparison to respective age and sex matched wild-type mice.

* denotes a level of statistical significance (Student's *t* test) of $p<0.05$. N.D. indicates very low or not expression (Ct value > 30) in the wild-type or *Agpat2*$^{-/-}$ liver.

Abbreviations: AGPAT, 1-acylglycerol-3-phosphate acyltransferase; GPAT, Glycerol-3-phosphate acyltransferase 1; ALCAT, Acyl-CoA:lysocardiolipin acyltransferase; LPEAT, Ethanolamine lysophospholipid acyltrasferase.

Footnote: Since publication of our paper with AGPAT8/ALCAT1 (Agarwal et al., 2006), Tang et al. (Tang et al., 2006) published a paper labeling NP_116106 as Agpat8 which has later been found to have GPAT activity (Cao et al., 2006) and was labeled as GPAT3. However, this AGPAT8/GPAT3 was not studied by us.

Table 3

Phenotypic comparison of male and female wild type and *Agpat2*$^{-/-}$ mice fed chow or a fat-free diet for two weeks

	Wild type				*Agpat2*$^{-/-}$			
Gender	**Male**		**Female**		**Male**		**Female**	
Diet	**Chow (6% fat)**	**Fat-free (0.2% fat)**	**Chow (6% fat)**	**Fat-free (0.2% fat)**	**Chow (6% fat)**	**Fat-free (0.2% fat)**	**Chow (6% fat)**	**Fat-free (0.2% fat)**
Number	6	5	4	4	5	6	4	5
Age, weeks	11–14	9.5–11.5	27–28	26–29	12–15	9.5–11.5	27–29	27–29
Body weight, g	28.3 ± 3.0	25.5 ± 3.9	21.9 ± 0.75	23.8 ± 1.6	28.7 ± 4.5	22.2 ± 5.0	22.3 ± 2.6	17.6 ± 0.36
Liver weight, g	1.50 ± 0.18	1.51 ± 0.20	0.98 ± 0.08	1.37 ± 0.29	4.56 ± 1.23	3.30 ± 1.16	3.60 ± 0.73	2.73 ± 0.25
Liver TG, mg/g	5.72 ± 1.6	16.8 ± 5.26	14.9 ± 4.1	29.0 ± 10	51.7 ± 18.4	22.6 ± 7.4†	49.3 ± 9.1	24.7 ± 9.3*
Plasma TG, mg/dL	100 ± 39	118 ± 31	68.0 ± 3.7	77.0 ± 28	194 ± 26	45.1 ± 105†	156 ± 101	41.2 ± 31.7$^{\#}$
Insulin, ng/mL	2.06 ± 1.06	2.70 ± 1.34	1.30 ± 0.062	1.82 ± 0.62	59.0 ± 36	79.6 ± 80	58.1 ± 11	40.3 ± 16
Glucose, mg/dL	255 ± 20	281 ± 19	297 ± 18	322 ± 41	591 ± 87	443 ± 156	425 ± 84	391 ± 141
Free fatty acids, meq/L	0.57 ± 0.19	0.63 ± 0.12	0.37 ± 0.06	0.34 ± 0.08	0.43 ± 0.09	0.21 ± 0.04†	0.37 ± 0.08	0.23 ± 0.05*

Wild type and *Agpat2*$^{-/-}$ mice of both sexes were fed ad libitum a rodent chow that contained 6.0% fat or a fat-free diet (0.2% fat) for 2 weeks. Each value represents the mean ± S.D.

$^{\#}$p=0.05,

*p<0.05;

†p<0.01; between the chow diet and the fat free diet for the same genotype and gender.